

# Surpassing Purely Digital Transmission: A Simplified Design of Hybrid Digital Analog Codes

Matthias Rüngeler and Peter Vary

Institute of Communication Systems and Data Processing ( **ivd** )

RWTH Aachen University, Germany

{ruengeler|vary}@ind.rwth-aachen.de

**Abstract**—One problem of conventional digital transmission systems that transmit real-valued source symbols is that the transmission fidelity always saturates for channels that have attained the design channel quality (worst-case channel condition); this saturation is caused by the irreversible error introduced by the source coder. Even though hybrid digital analog (HDA) codes address this problem by additionally transmitting the inherent quantization error by using analog methods, the design and the decoding of these HDA codes is complex or even impossible for long block lengths. Thus, the aim of this study is to introduce a new way to design HDA codes using well-known digital codes. Another objective is to theoretically and empirically compare the proposed design with the conventional purely digital transmission systems. This study applied Monte Carlo simulations with Reed-Solomon codes or convolutional codes as the digital part and LMMSE estimation in the analog part of the HDA system. The simulation results agreed well with the theoretical considerations. Since the proposed design uses well-established, excellent digital codes that support long block lengths, the design and decoding of HDA codes is simplified. The inherent error introduced by the source coder is reduced by combining these digital codes with analog transmission, thereby eliminating the saturation of the transmission fidelity. The newly proposed HDA system surpasses the purely digital transmission system at all channel qualities.

**Index Terms**—Hybrid Digital Analog (HDA), Reed-Solomon code, convolutional code, LMMSE estimator, joint MMSE decoding

## I. INTRODUCTION

Consider the problem of transmitting real-valued source symbols or source parameters over a Gaussian channel. The source-channel separation principle [1] leads to the common solution: separate digital source coding with binary representation of the source symbols and digital channel coding. These transmission systems are excellent at the design channel quality which is usually the worst-case channel condition, e.g. at the cell edge of a radio system. One drawback of this solution, however, is often ignored: If the receiver experiences a better channel quality (cSNR) than the transmission system is designed for, the transmission fidelity i.e. signal-to-noise ratio (pSNR) does not exceed the design transmission fidelity and, thus, it saturates. This saturation is caused by the inherent error introduced by the digital source coder which, even in the case of error-free transmission of the coded bits, can never be compensated for. Skoglund et al. [2] call this saturation the *level-off effect*, a characteristic of purely digital transmission systems. In contrast, analog transmission systems working with continuous-amplitude processing do not show this adverse characteristic. For increased channel qualities, the transmission fidelity improves, which is referred to as *graceful improvement*.

Such systems showing *graceful improvement* can be applied in all fields where real-valued source symbols or source parameters are transmitted over channels having a higher channel quality at particular times or locations than dictated by the given design. Examples are systems with different channel qualities for different receivers and systems with fast changing channel quality which prevents revealing the current channel quality to the transmitter. Other applications involve systems with inexpensive transmitters not designed to adapt to changing channels, e.g. transmitters used in wireless microphones or headsets and wireless sensors.

Several purely analog transmission systems working with different approaches, e.g. chaotic dynamical systems, Archimedes spirals, orthogonal polynomials or shift maps [3], [4], [5], [6] have been proposed. They all show *graceful improvement* of the transmission fidelity. Usually these systems work well for very small block sizes. For larger block sizes, however, the design is too complex or shows poor performance. The theory of combining digital and analog coding, the so-called hybrid digital analog (HDA) coding, has been proposed and analyzed in several papers, e.g. [7], [8], [9]. There, the benefits of both the digital and the analog world are exploited. A digital code, for example, yields asymptotical optimal performance at the design channel quality for infinite block lengths, whereas an analog coding system ensures *graceful improvement* for better channels. Another way to transmit, e.g., speech signals using mixed analog digital processing is analyzed in [10]. The spectral envelope is transmitted digitally, and the prediction error is transmitted using continuous-amplitude processing.

Skoglund et al. [2] proposed and analyzed a HDA system with finite block sizes by using vector quantization and general channel coding as the digital part and uncoded transmission of the quantization errors as the analog part. The digital and analog channel symbols are multiplexed and transmitted over an additive white Gaussian noise (AWGN) channel. Their system is designed for error control by using more real channel symbols  $N$  than real source symbols  $M$ . The vector quantizer, the decoder codebook at the transmitter side (to calculate the quantization error), the decoder codebook at the receiver side, the general channel code and normalization factors for the analog part are optimized jointly using numerical methods. For an 8-dimensional Gaussian vector source whose symbols are transmitted with 16 channel symbols, Monte Carlo simulations prove the superiority of the HDA system over a purely digital system which uses the same numerical optimization strategy.

Nonetheless, the aforementioned system has drawbacks: the design of the HDA codes is complex or even impossible

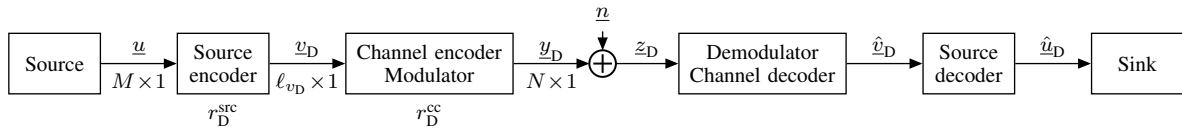


Fig. 1. Purely digital transmission system.

for long block lengths. Additionally, exhaustive search in the decoding algorithms is required for the general vector quantization and general digital channel coding.

To address these problems, this current study introduces a new design for HDA systems using well-known digital source and channel coding. The proposed design is theoretically and empirically examined and is compared to the conventional purely digital transmission systems. This paper first introduces the HDA system and then gives a theoretical analysis of its performance and provides design guidelines. Finally, Monte Carlo simulations are conducted.

## II. SYSTEM MODEL

Figure 1 shows a conventional digital transmission system. The source emits continuous-amplitude and discrete-time source symbols  $\underline{u}$  with dimension  $M \times 1$  following the probability density function (pdf)  $p_{\underline{u}}$ . Then, a source coder encodes the source vector to  $\ell_{v_D}$  source bits, yielding the vector  $\underline{v}_D$ . The rate  $r_D^{\text{src}} = M/\ell_{v_D}$  describes the ratio between the source dimension and the number of bits. Subsequently, a digital channel code followed by digital modulation transforms the source bits into  $N$  real-valued symbols forming the vector  $\underline{y}_D$  with  $E\{y_D^2\} = 1$ . Modulation schemes using complex-valued symbols (e.g. QPSK, 8PSK) are also considered by noting the equivalence between one complex symbol and two real symbols. The ratio between the number of bits  $\ell_{v_D}$  and the number of real symbols  $N$  is denoted by  $r_D^{\text{cc}} = \ell_{v_D}/N$ . Moreover, the ratio between the number of real channel symbols and real source symbols is given by  $r_D = r_D^{\text{src}} \cdot r_D^{\text{cc}} = M/N$ . However, additive white Gaussian noise  $\underline{n}$  with variance  $\sigma_n^2$  per dimension disturbs the channel symbols, thereby yielding the received symbols  $\underline{z}_D$ . The channel quality is denoted by  $\text{cSNR} = E\{y^2\}/\sigma_n^2$ . After demodulation, channel and source decoding,  $\hat{\underline{u}}_D$  gives an estimate of the initial source symbols  $\underline{u}$ .

Figure 2 illustrates the proposed simplified HDA transmission system. The general idea here is to use a conventional digital transmission system and additionally transmit the error introduced by the conventional source coder by using continuous-amplitude processing. The upper branch of the hybrid encoder and decoder is referred to as the *digital* part and the lower branch as the *analog* part. The digital part is a

purely digital transmission system; the number of real channel dimensions used by the digital part is denoted by  $D$ . The analog part utilizes  $A > 0$  channel uses. Thus, the number of channel uses in the HDA system is:

$$N = D + A. \quad (1)$$

Thus,  $D < N$ . In order to compare both systems, the respective numbers of channel uses ( $N$ ) in the digital system and in the HDA system are equal.

In the hybrid encoder, the source decoder converts the source bits  $\underline{v}_H$  to a quantized source representation  $\underline{u}_H^d$ . The distortion introduced by the conventional source coder  $\underline{u}_H^a = \underline{u} - \underline{u}_H^d$  is processed in the analog branch. The analog mapper uses continuous-amplitude processing to map the vector  $\underline{u}_H^a$  to the vector  $\underline{y}_H^a$  with length  $A$  and average energy  $E\{(y_H^a)^2\} = 1$ :

$$\underline{y}_H^a = \sqrt{\frac{1}{E\{(f(\underline{u}_H^a))^2\}}} \cdot f(\underline{u}_H^a). \quad (2)$$

The ratio between the input and the output dimensions of the block is  $r_H^{\text{mapp}} = M/A$ . This mapping  $f(\cdot)$  could, e.g., be a linear amplification or a nonlinear function with a rate of  $r_H^{\text{mapp}} = 1$  or an Archimedes Spiral [4] which maps one symbol onto two symbols ( $r_H^{\text{mapp}} = 1/2$ ).

After multiplexing the symbols from the digital and analog branch and transmitting over the AWGN channel, the symbols are demultiplexed and conveyed to the digital and analog decoding branches. The analog demapper then estimates the original quantization error  $\underline{u}_H^a$  which can be facilitated using several methods such as maximum likelihood (ML), maximum a posteriori (MAP), linear minimum mean square error (LMMSE) and minimum mean square error (MMSE) estimators. The outputs of the analog and digital branches are added, whereby  $\hat{\underline{u}}_H$  gives an estimate of the initial source symbols.

Unlike the HDA system considered by Skoglund et al. [2], the source decoder used in the receiver and transmitter are the same (see Fig. 2). Moreover, well-known digital codes are used for channel coding. The normalization factors  $\alpha$  and  $\beta$  used by Skoglund et al. in the analog part are generalized to a nonlinear mapping (analog mapper in Fig. 2) which also allows error correction in the analog branch (e.g. 1:2 mapping).

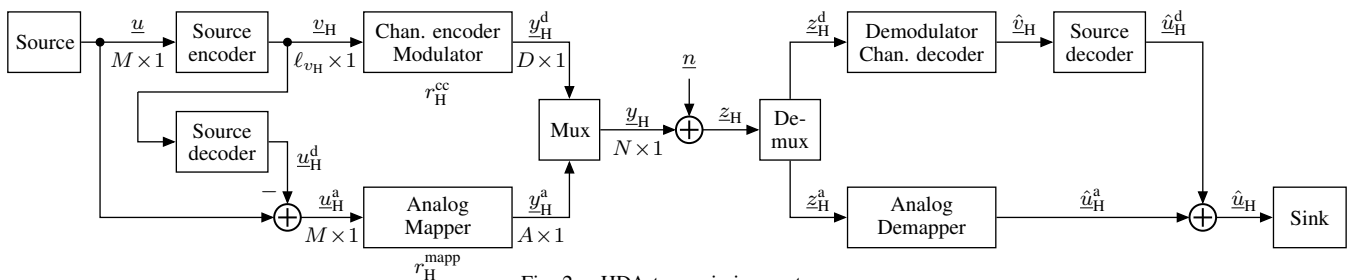


Fig. 2. HDA transmission system.

### III. OPTIMAL DECODING

In Fig. 2, two separate decoders are used for the digital and the analog part, and the decoding results are added. Even though this design is intended to be simpler, the question remains whether this design is optimal.

In the following, a joint MMSE estimator is derived, which does not necessarily use separate estimation for the analog and digital parts. The effect of the source coder is denoted by  $\underline{u}_H^d = Q(\underline{u})$ , where  $Q(u)$  refers to, a mere quantizer or more complex source coding. The channel transition probabilities for the digital and analog part are given by  $p_{\underline{z}_H^d|\underline{u}_H^d}$  and  $p_{\underline{z}_H^a|\underline{u}_H^a}$  with  $\underline{z}_H$  denoting random processes. The *a posteriori* probability of the source  $\underline{u}$ , given the received values of the digital  $\underline{z}_H^d$  and analog  $\underline{z}_H^a$  channel, can be derived as follows (see Appendix for complete derivation):

$$p_{\underline{u}|\underline{z}_H^a, \underline{z}_H^d}(\underline{u}|\underline{z}_H^a, \underline{z}_H^d) = \frac{1}{C} \cdot p_{\underline{z}_H^a|\underline{u}_H^a}(\underline{z}_H^a|\underline{u} - Q(\underline{u})) \cdot p_{\underline{z}_H^d|\underline{u}_H^d}(\underline{z}_H^d|Q(\underline{u})) \cdot p_{\underline{u}}(\underline{u}). \quad (3)$$

The constant  $C$  normalizes  $p_{\underline{u}|\underline{z}_H^a, \underline{z}_H^d}$ , so it integrates to 1. The MMSE estimator can directly be stated as a conditional expectation:

$$\hat{\underline{u}} = E_{\underline{u}|\underline{z}_H^a, \underline{z}_H^d}(\underline{u}|\underline{z}_H^a, \underline{z}_H^d) = \int \underline{u} \cdot p_{\underline{u}|\underline{z}_H^a, \underline{z}_H^d}(\underline{u}|\underline{z}_H^a, \underline{z}_H^d) d\underline{u}. \quad (4)$$

Equations (3) and (4) show that the general MMSE estimator cannot be calculated using separate estimators for the digital and analog parts. However, if statistical independence between quantization levels  $\underline{u}_H^d$  and the quantization error  $\underline{u}_H^a$  is assumed, which is exactly given, e.g., for sources with a uniform pdf and using a uniform quantizer and asymptotically given for other sources and quantizers, the following relation holds:

$$p_{\underline{u}_H^a, \underline{u}_H^d}(\underline{u}_H^a, \underline{u}_H^d) = p_{\underline{u}_H^a}(\underline{u}_H^a) \cdot p_{\underline{u}_H^d}(\underline{u}_H^d). \quad (5)$$

Under this assumption, the MMSE estimator can be stated as (see Appendix):

$$\hat{\underline{u}}_H = \hat{\underline{u}}_H^a + \hat{\underline{u}}_H^d. \quad (6)$$

Equation 6 shows that, given statistical independence (5), independent MMSE estimation in the digital and analog parts and adding up the results yield the optimal MMSE estimation. In the following, independent estimation is used. The digital part employs digital channel decoders which, in the best-case scenario, is a ML estimation. The analog part uses LMMSE estimation by inverting the effect of (2) and weighting with  $c\text{SNR}/(1 + c\text{SNR})$  to seeks the minimum mean square error which can be achieved using linear methods [11].

### IV. SYSTEM PROPERTIES

The signal-to-noise performance  $\text{pSNR}_H$  of the HDA transmission system is influenced by the distortion in the analog part and the distortion in the digital part. If (5) is valid, the variance of the distortions of the two parts can be added:

$$\begin{aligned} \text{pSNR}_H &= \frac{\sigma_{\underline{u}}^2}{E\{(\underline{u} - \hat{\underline{u}}_H)^2\}} \\ &= \frac{\sigma_{\underline{u}}^2}{E\{(\underline{u}_H^a - \hat{\underline{u}}_H^a)^2\} + E\{(\underline{u}_H^d - \hat{\underline{u}}_H^d)^2\}}. \end{aligned} \quad (7)$$

#### A. Bad Channel Conditions

In the case of bad channel conditions, the digital channel decoder cannot decode error freely anymore and the high bit error rate (BER) after channel decoding causes the digital part to contribute to the overall distortion. Even though, the analog part is also disturbed heavily, but using a LMMSE estimator, the distortion in the analog part can be upper bounded by the variance of the quantization noise  $E\{(\underline{u}_H^a - \hat{\underline{u}}_H^a)^2\} \leq \sigma_{\underline{u}_H^a}^2$  [11] yielding

$$\text{pSNR}_H \geq \frac{\sigma_{\underline{u}}^2}{\sigma_{\underline{u}_H^a}^2 + E\{(\underline{u}_H^d - \hat{\underline{u}}_H^d)^2\}} = \frac{\sigma_{\underline{u}}^2}{E\{(\underline{u} - \hat{\underline{u}}_H^d)^2\}} \quad (8)$$

with  $\sigma_{\underline{u}_H^a}^2 = E\{(\underline{u} - \underline{u}_H^d)^2\}$ . The right side of (8) equals the system performance of just the digital part of the HDA system. Hence, the performance-bound (8) only depends on the transmission errors in the digital part.

Upon uniformly quantizing source symbols with a uniform pdf and disturbing the quantization bits with a certain nonzero BER, the overall mean square error (MSE) is independent of the fidelity of the quantizer, and only depends on the BER [12, p. 293]; see also Fig. 3. Thus, lowering the BER after digital channel decoding by employing stronger digital channel codes (e.g. with a lower coding rate) reduces the MSE. Consequently, when transmission errors in the digital part contribute to the overall distortion of the source symbols, the  $\text{pSNR}_H$  of a HDA system is superior or equal to the  $\text{pSNR}_D$  of a purely digital system, provided that the coding rate of the digital channel code for the HDA system is lower than that for the purely digital system:

$$r_D^{\text{cc}} \geq r_H^{\text{cc}}. \quad (9)$$

Since the HDA system needs equal or lower coding rates for the digital part and  $A$  additional channel uses for the analog part, the same number of channel uses ( $N$ ) in both systems can only be achieved by changing another parameter: the number of bits ( $\ell_{v_H}$ ) generated by the source encoder. This number of bits has to be decreased by reducing the fidelity of the quantizer in the HDA system.

The quantizer in the purely digital transmission system utilizes  $F_D = \ell_{v_D}/M = r_D^{\text{cc}} \cdot N/M$ , and the quantizer in the HDA system utilizes  $F_H = \ell_{v_H}/M = r_H^{\text{cc}} \cdot (N - A)/M$  quantization bits per source dimension. Starting with (9), the difference in quantization bits per dimension  $\Delta F$  can be calculated as follows:

$$\begin{aligned} &r_D^{\text{cc}} \geq r_H^{\text{cc}} \\ \Leftrightarrow &\frac{F_D \cdot M}{N} \geq \frac{F_H \cdot M}{N - A} \\ \Leftrightarrow &F_D \geq F_H \cdot \left(1 + \frac{A}{N - A}\right) \\ \Leftrightarrow &\Delta F := F_D - F_H \geq F_H \cdot \frac{A}{N - A} \cdot \frac{M}{M} \\ \Leftrightarrow &\Delta F \geq \frac{r_D^{\text{cc}}}{r_H^{\text{cc}}} \cdot \frac{A}{M}. \end{aligned} \quad (10)$$

As long as the condition (10) is met, the HDA system performance surpasses or equals that of the purely digital system for channels with transmission errors in the digital part that contribute to the overall distortion.

## B. Good Channel Conditions

Now, the case of good channels yielding error-free transmission in the digital part is considered. Consequently, the fidelity has saturated and the distortion in the digital part is zero  $E\{(\underline{u}_H^d - \hat{\underline{u}}_H^d)^2\} = 0$  and with

$$\text{pSNR}_H^a = \frac{\sigma_{\underline{u}_H^a}^2}{E\{(\underline{u}_H^a - \hat{\underline{u}}_H^a)^2\}}, \quad (11)$$

Eq. (7) can be reformulated to:

$$\text{pSNR}_{H, \text{ sat.}} = \frac{\sigma_{\underline{u}}^2}{E\{(\underline{u}_H^a - \hat{\underline{u}}_H^a)^2\}} = \frac{\sigma_{\underline{u}}^2}{\sigma_{\underline{u}_H^a}^2} \cdot \text{pSNR}_H^a. \quad (12)$$

The fraction  $(\sigma_{\underline{u}}^2/\sigma_{\underline{u}_H^a}^2)$  in (12) refers to the pSNR of the digital source code (quantization noise) and  $\text{pSNR}_H^a$  refers to the pSNR of just the analog part. Hence, for channels with no transmission errors in the digital part, the overall performance only depends on the analog part and the fidelity of the quantizer.

Since less bits in the HDA transmission system are spent for the quantization (10), the variance of the quantization noise is higher than that of the purely digital system. This loss has to be compensated for by the analog part of the HDA system.

In the following derivation, the rate distortion function for Gaussian sources with rate  $R_H^d$  for the quantizer in the HDA case and  $R_D^d$  for the purely digital case is used with a loss factor ( $R_{\text{imp}}^d$ ) that accounts for other source pdfs and quantizer imperfection. The loss factor is assumed to be equal for quantizers with different rates, since they operate on the same  $M$  dimensional vectors  $\underline{u}$  (same space filling advantage and same shape advantage [13]). This way, the 6 dB-per-bit rule and the  $\text{pSNR}_H^a$ , which needs to be achieved in the analog part to compensate for the quantizer with lower fidelity, are derived:

$$\begin{aligned} \text{pSNR}_{H, \text{ sat.}} &\geq \text{pSNR}_{D, \text{ sat.}} \\ \Leftrightarrow 2^{2 \cdot (R_H^d - R_{\text{imp}}^d)} \cdot \text{pSNR}_H^a &\geq 2^{2 \cdot (R_D^d - R_{\text{imp}}^d)} \\ \Leftrightarrow \text{pSNR}_H^a &\geq 4^{R_D^d - R_H^d} = 4^{\Delta F} \end{aligned} \quad (13)$$

$$\Leftrightarrow 10 \log_{10}(\text{pSNR}_H^a) \geq \Delta F \cdot 6 \text{ dB}. \quad (14)$$

The channel quality with error-free transmission in the digital part can be bounded using the Shannon capacity. A source encoder which yields output bits with entropy 1 and an ideal channel code are assumed. This assumption facilitates error-free decoding employing  $r_D^{\text{cc}} \leq C$  bits per channel use at  $\text{cSNR}_D^{\text{sat.}}$ :

$$\begin{aligned} r_D^{\text{cc}} \leq C &= \frac{1}{2} \text{ld}(1 + \text{cSNR}_D^{\text{sat.}}) \\ \Leftrightarrow \text{cSNR}_D^{\text{sat.}} &\geq 4^{r_D^{\text{cc}}} - 1 \end{aligned} \quad (15)$$

$$\Leftrightarrow \text{cSNR}_D^{\text{sat.}} \cdot \Delta_{\text{loss}} = 4^{r_D^{\text{cc}}} - 1. \quad (16)$$

The factor  $\Delta_{\text{loss}}$  equals 1 for ideal digital channel codes, and  $0 < \Delta_{\text{loss}} < 1$  holds for codes in practice.

Eqs. (10) and (13) are now combined to calculate the performance requirement in terms of  $\text{pSNR}_H^a$  of the analog

part at the channel quality at which the digital part saturates such that a HDA system surpasses a purely digital system:

$$\text{pSNR}_H^a \geq 4^{\Delta F} \geq 4^{\frac{r_D^{\text{cc}}}{r_H^{\text{mapp}}}} = \left(4^{r_D^{\text{cc}}}\right)^{\frac{1}{r_H^{\text{mapp}}}}. \quad (17)$$

Combining (17) with (16), the required performance of the analog part at  $\text{cSNR}_D^{\text{sat.}} \cdot \Delta_{\text{loss}}$  is:

$$\text{pSNR}_H^a \geq (\text{cSNR}_D^{\text{sat.}} \cdot \Delta_{\text{loss}} + 1)^{\frac{1}{r_H^{\text{mapp}}}}. \quad (18)$$

Furthermore, the maximum  $\text{pSNR}_H^a$  which can be achieved according to the channel capacity and rate distortion functions is described by the *optimum performance theoretically attainable* (OPTA). For transmitting  $M$  Gaussian source symbols employing  $A = M/r_H^{\text{mapp}}$  channel uses, OPTA can be stated as follows and cannot be exceeded:

$$\text{OPTA} := (\text{cSNR} + 1)^{\frac{1}{r_H^{\text{mapp}}}} \geq \text{pSNR}_H^a. \quad (19)$$

For an ideal digital code,  $\Delta_{\text{loss}} = 1$  holds. Subsequently combining (18) and (19) infers that inequalities (18) and (17) have to hold with equality. This implies that  $r_H^{\text{cc}} = r_D^{\text{cc}}$  and therefore  $\Delta F = r_D^{\text{cc}}/r_H^{\text{mapp}}$  and that the analog part reaches OPTA at  $\text{cSNR}_D^{\text{sat.}}$ .

There is an analog system known to reach (19) for finite block lengths: a linear encoder ( $f(\underline{u}_H^a) = \underline{u}_H^a$ ) with no additional redundancy ( $r_H^{\text{mapp}} = 1$ ) and a LMMSE estimator at the receiver that knows about the current channel quality (cSNR). The performance of the LMMSE estimator is [11]

$$\text{pSNR}_H^a = \text{cSNR} + 1, \quad (20)$$

and, consequently, (18) holds with equality. Thus, it is possible, even for ideal digital codes, to design a HDA system which surpasses a purely digital system for all channel qualities. For quantization noise which does not follow a Gaussian pdf, OPTA is higher and e.g. a MMSE estimator exceeds the performance of the LMMSE estimator and, therefore, can further improve the performance of the HDA system.

In the case of practical nonideal digital codes,  $0 < \Delta_{\text{loss}} < 1$  holds and (17) and (18) do not need to hold with equality anymore. This implies that in the analog part, systems with  $r_H^{\text{mapp}} \neq 1$  can be used which do not reach OPTA and that the design of the quantizer for the HDA system is more flexible, since  $\Delta F$  does not have to exactly match  $r_D^{\text{cc}}/r_H^{\text{mapp}}$ . However, by deviating too much from equality, the performance gain of the HDA system shrinks or even may be negative.

For ideal channel codes, a transition region between no errors in the digital part and a lot of errors and thus a nonzero distortion in the digital part does not exist, since the breakdown of the digital code is abrupt. For practical codes with  $0 < \Delta_{\text{loss}} < 1$ , the transition region widens and two cases can be distinguished: For  $r_D^{\text{cc}} = r_H^{\text{cc}}$ ,  $r_H^{\text{mapp}} = 1$  and a LMMSE estimator, the HDA code surpasses the purely digital system for  $\text{cSNR} \geq \text{cSNR}_D^{\text{sat.}}$ . By contrast, in the region where the digital part contributes to the overall distortion, the performance of HDA and digital systems is equal. Here, a slight transition can be observed between the region of errors in the digital part and the region where the digital code decodes error-free. Thus, the HDA code surpasses the purely digital system.

For  $r_D^{cc} > r_H^{cc}$ , the proposed HDA system surpasses the purely digital system for bad channels. However  $\Delta F > r_D^{cc}/r_H^{mapp}$  and, hence, the performance of the analog part  $pSNR_H^a$  (13) needs to be higher, too. The  $pSNR_H^a$  may not suffice for channel qualities at which the digital code of the purely digital system has already saturated. In this case, the purely digital system might surpass the HDA system in this transition region. Nonetheless, the performance of the proposed HDA code improves with better channels and eventually surpasses that of a purely digital system.

## V. SIMULATION RESULTS

Figure 3 shows the performance of a HDA system and of two purely digital systems without digital channel coding. One ( $M = 1$ ) source symbol following a uniform pdf is uniformly quantized either with 5 or 6 bits and then transmitted using BPSK modulation with or without the quantization error as an additional channel symbol. The purely digital system using  $F_D = 6$  bits saturates at  $pSNR_{D, sat.} = 36$  dB. The digital system employing one bit less ( $F_D = 5$ ) saturates at 30 dB following the 6 dB-per-bit rule. Additionally, transmitting the quantization error ( $A = 1$ ) using linear processing  $f(\underline{u}_H^a) = \underline{u}_H^a$  (see (2)) and a LMMSE estimator at the receiver yields the HDA system with  $F_H = 5$ . Compared to the purely digital system with  $F_D = 5$ , the performance of the proposed HDA system ( $F_H = 5$ ) improves according to (20) and also surpasses the performance of the purely digital system with  $F_D = 6$  for all channel qualities. Both the HDA system with  $F_H = 5$  and the purely digital system with  $F_D = 6$  employ  $N = 6$  channel uses and therefore they can be compared. Since no digital channel coding is applied, the BER is the same for all three systems. For bad channels, where the BER is nonzero, the performance of all three systems is also the same, independent of the fidelity of the quantizer (Sec. IV-A).

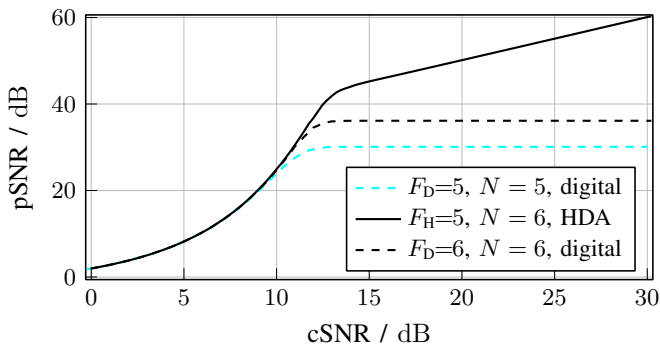


Fig. 3. HDA and digital transmission without digital channel coding. Uniform source pdf.  $M = 1$ . HDA:  $A = 1$ ,  $D = 5$ ,  $N = 6$ . Digital:  $N \in \{5, 6\}$ .

In the following, digital channel coding is applied. Since digital codes do not perform well for the quantization bits of only one source symbol, the dimension of the input vector  $\underline{u}$  is moderately increased to  $M = 8$ . In addition, the channel dimension is set to  $N = 56$  for all simulations to permit comparison of the HDA and digital systems. As in the first example,  $f(\underline{u}_H^a) = \underline{u}_H^a$  and a LMMSE estimator are used.

Figure 4 illustrates the performance of HDA and digital transmission systems using a uniform source pdf, uniform quantization and Reed-Solomon (RS) codes performing on

GF(4). Depending on the coding rate, the corresponding code is a  $(p,q)$ -RS code with  $p = 15$  and  $q \in \{5, 9, 13\}$  shortened by 1 or 3 symbols. For decoding, a hard-decision Berlekamp-Massey algorithm is applied. These simulations reveal that for all quantization fidelities, the HDA code employing quantization with lower fidelity surpasses the corresponding purely digital code for all channel qualities.

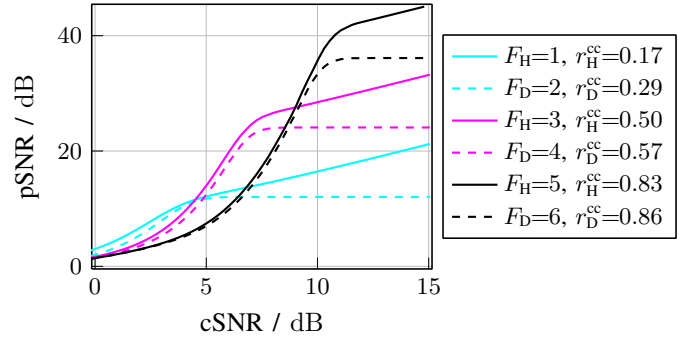


Fig. 4. HDA and digital transmission using Reed-Solomon codes. Uniform source pdf.  $M = 8$ . HDA:  $A = 8$ ,  $D = 48$ ,  $N = 56$ . Digital:  $N = 56$ .

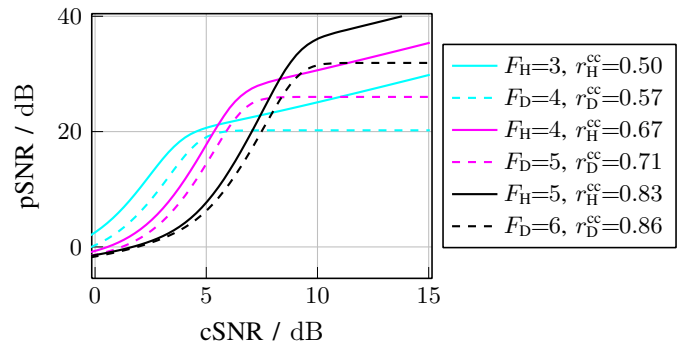


Fig. 5. HDA and digital transmission using convolutional codes. Gaussian source pdf.  $M = 80$ . HDA:  $A = 80$ ,  $D = 480$ ,  $N = 560$ . Digital:  $N = 560$ .

Figure 5 shows simulation results for a Gaussian source with  $M = 80$  with scalar Lloyd-Max quantization and a rate- $\frac{1}{2}$  recursive systematic convolutional code with the generator polynomial  $\{1, 15/13\}_8$  — the same code which is used in UMTS-LTE. The different rates for different quantizer fidelities are achieved by puncturing only the parity bits, thereby yielding  $N = 560$ . Zero termination results in tail bits which are also transmitted and never punctured. These codes perform better for this application than the Reed-Solomon codes. This may be attributed to the MAP decoder which has an advantage over the employed hard-decision Berlekamp-Massey algorithm, because reliability information from the channel is exploited. Also here, the proposed HDA system surpasses the corresponding purely digital transmission system for all channel qualities.

## VI. CONCLUSION

This paper has introduced a new way to design hybrid digital analog (HDA) transmission systems using well-established digital codes. A key aspect here is to apply a quantizer with lower fidelity for the HDA system than that used in a purely digital system. Another important aspect is to also transmit the quantization error using analog methods while keeping the overall number of channel uses constant.

Since this proposed design employs well-known, excellent digital codes, long block lengths can be supported. Thus, the design in decoding HDA codes has been simplified. Moreover, the inherent error introduced by the source coder is reduced by combining these digital codes with analog transmission, thereby eliminating the saturation of the transmission fidelity.

Furthermore, a joint MMSE estimation at the decoder has been derived. It has been proven that independent decoding of the digital and the analog parts is still optimal for statistically independent quantization levels and quantization errors.

Simulations comparing purely digital and HDA transmission systems employing uniform and Gaussian source pdfs, Reed-Solomon and convolutional codes show the superiority of HDA codes over purely digital codes for all channel qualities. These simulations also indicate that the performance of HDA codes rises for increasing channel qualities (*graceful improvement*). Ultimately, the proposed HDA transmission system surpasses the purely digital transmission system at all channel qualities.

## APPENDIX

The *a posteriori* probability of  $\underline{u}$  (3) can be derived using the following steps with  $C = p_{\underline{z}^a, \underline{z}^d}(\underline{z}^a, \underline{z}^d)$ <sup>1</sup>:

$$\begin{aligned} p_{\underline{u}|\underline{z}^a, \underline{z}^d}(\underline{u}|\underline{z}^a, \underline{z}^d) &= \frac{1}{C} \cdot p_{\underline{u}, \underline{z}^a, \underline{z}^d}(\underline{u}, \underline{z}^a, \underline{z}^d) \\ &= \frac{1}{C} \cdot p_{\underline{z}^a, \underline{z}^d|\underline{u}, \underline{u}^a, \underline{u}^d}(\underline{z}^a, \underline{z}^d, \underline{u}|\underline{u} - Q(\underline{u}), Q(\underline{u})) \\ &= \frac{1}{C} \cdot p_{\underline{z}^a|\underline{z}^d, \underline{u}, \underline{u}^a, \underline{u}^d}(\underline{z}^a|\underline{z}^d, \underline{u}, \underline{u} - Q(\underline{u}), Q(\underline{u})) \\ &\quad \cdot p_{\underline{z}^d|\underline{u}, \underline{u}^a, \underline{u}^d}(\underline{z}^d|\underline{u}, \underline{u} - Q(\underline{u}), Q(\underline{u})) \\ &\quad \cdot p_{\underline{u}|\underline{u}^a, \underline{u}^d}(\underline{u}|\underline{u} - Q(\underline{u}), Q(\underline{u})) \\ &= \frac{1}{C} \cdot p_{\underline{z}^a|\underline{u}^a}(\underline{z}^a|\underline{u} - Q(\underline{u})) \cdot p_{\underline{z}^d|\underline{u}^d}(\underline{z}^d|Q(\underline{u})) \cdot p_{\underline{u}}(\underline{u}). \end{aligned}$$

To derive (6), some prerequisite are needed:

For handling both digital and analog values together,  $\tilde{p}$  is defined as

$$\tilde{p}_{\underline{u}^a, \underline{u}^d}(\underline{u}^a, \underline{u}^d) \cdot \delta(Q(\underline{u}^d) - \underline{u}^d) = p_{\underline{u}^a, \underline{u}^d}(\underline{u}^a, \underline{u}^d). \quad (21)$$

The channel transition probabilities are independent for independent AWGN channels:

$$p_{\underline{z}^a, \underline{z}^d|\underline{u}^a, \underline{u}^d}(\underline{z}^a, \underline{z}^d|\underline{u}^a, \underline{u}^d) = p_{\underline{z}^a|\underline{u}^a}(\underline{z}^a|\underline{u}^a) \cdot p_{\underline{z}^d|\underline{u}^d}(\underline{z}^d|\underline{u}^d). \quad (22)$$

Later on, statistical independence between  $\underline{u}^a$  and  $\underline{u}^d$  is assumed:

$$\tilde{p}_{\underline{u}^a, \underline{u}^d}(\underline{u}^a, \underline{u}^d) = p_{\underline{u}^a}(\underline{u}^a) \cdot P_{\underline{u}^d}(\underline{u}^d). \quad (23)$$

If  $\underline{u}^a$  and  $\underline{u}^d$  are statistically independent, the same holds true for  $\underline{z}^a$  and  $\underline{z}^d$ :

$$p_{\underline{z}^a, \underline{z}^d}(\underline{z}^a, \underline{z}^d) = p_{\underline{z}^a}(\underline{z}^a) \cdot p_{\underline{z}^d}(\underline{z}^d). \quad (24)$$

In general, the pdf  $p_{\underline{u}}(\underline{u})$  of a sum of two values can be written as :

$$\begin{aligned} p_{\underline{u}}(\underline{u}) &= \int p_{\underline{u}^a, \underline{u}^d}(\underline{u} - \underline{u}^d, \underline{u}^d) d\underline{u}^d \\ &\stackrel{(21)}{=} \int \tilde{p}_{\underline{u}^a, \underline{u}^d}(\underline{u} - \underline{u}^d, \underline{u}^d) \cdot \delta(Q(\underline{u}^d) - \underline{u}^d) d\underline{u}^d \\ &= \sum_{\underline{u}^d} \tilde{p}_{\underline{u}^a, \underline{u}^d}(\underline{u} - \underline{u}^d, \underline{u}^d). \end{aligned} \quad (25)$$

<sup>1</sup>To improve readability, the index H is omitted in the Appendix.

The *a posteriori* pdf can therefore be written as

$$\begin{aligned} p_{\underline{u}|\underline{z}^a, \underline{z}^d}(\underline{u}|\underline{z}^a, \underline{z}^d) &= \sum_{\underline{u}^d} \tilde{p}_{\underline{u}^a, \underline{u}^d|\underline{z}^a, \underline{z}^d}(\underline{u} - \underline{u}^d, \underline{u}^d|\underline{z}^a, \underline{z}^d) \\ &= \sum_{\underline{u}^d} \frac{p_{\underline{z}^a, \underline{z}^d|\underline{u}^a, \underline{u}^d}(\underline{z}^a, \underline{z}^d|\underline{u} - \underline{u}^d, \underline{u}^d) \cdot \tilde{p}_{\underline{u}^a, \underline{u}^d}(\underline{u} - \underline{u}^d, \underline{u}^d)}{p_{\underline{z}^a, \underline{z}^d}(\underline{z}^a, \underline{z}^d)} \\ &\stackrel{(22), (23)}{=} \frac{1}{C} \sum_{\underline{u}^d} p_{\underline{z}^a|\underline{u}^a}(\underline{z}^a|\underline{u} - \underline{u}^d) \cdot p_{\underline{u}^a}(\underline{u} - \underline{u}^d) \cdot p_{\underline{z}^d|\underline{u}^d}(\underline{z}^d|\underline{u}^d) \cdot P_{\underline{u}^d}(\underline{u}^d) \\ &= \frac{1}{C} \sum_{\underline{u}^d} p_{\underline{z}^a, \underline{u}^a}(\underline{z}^a, \underline{u} - \underline{u}^d) \cdot \tilde{p}_{\underline{z}^d, \underline{u}^d}(\underline{z}^d, \underline{u}^d). \end{aligned} \quad (26)$$

Now, the MMSE estimate  $\hat{\underline{u}}$  of  $\underline{u}$  can be stated:

$$\begin{aligned} \hat{\underline{u}} &= \int \underline{u} \cdot p_{\underline{u}|\underline{z}^a, \underline{z}^d}(\underline{u}|\underline{z}^a, \underline{z}^d) d\underline{u} \\ &\stackrel{(26), (24)}{=} \int \sum_{\underline{u}^d} \underline{u} \cdot \frac{p_{\underline{z}^a, \underline{u}^a}(\underline{z}^a, \underline{u} - \underline{u}^d)}{p_{\underline{z}^a}(\underline{z}^a)} \cdot \frac{\tilde{p}_{\underline{z}^d, \underline{u}^d}(\underline{z}^d, \underline{u}^d)}{p_{\underline{z}^d}(\underline{z}^d)} d\underline{u} \\ &= \sum_{\underline{u}^d} \left( \int \underline{u} \cdot p_{\underline{u}|\underline{z}^a}(\underline{u} - \underline{u}^d|\underline{z}^a) d\underline{u} \right) \cdot P_{\underline{u}^d|\underline{z}^d}(\underline{u}^d|\underline{z}^d) \\ &= \sum_{\underline{u}^d} \left( \int (\underline{u}^a + \underline{u}^d) \cdot p_{\underline{u}|\underline{z}^a}(\underline{u}^a|\underline{z}^a) d\underline{u}^a \right) \cdot P_{\underline{u}^d|\underline{z}^d}(\underline{u}^d|\underline{z}^d) \\ &= \sum_{\underline{u}^d} (\hat{\underline{u}}^a + \underline{u}^d) \cdot P_{\underline{u}^d|\underline{z}^d}(\underline{u}^d|\underline{z}^d) \\ &= \hat{\underline{u}}^a \cdot \sum_{\underline{u}^d} P_{\underline{u}^d|\underline{z}^d}(\underline{u}^d|\underline{z}^d) + \sum_{\underline{u}^d} \underline{u}^d \cdot P_{\underline{u}^d|\underline{z}^d}(\underline{u}^d|\underline{z}^d) = \hat{\underline{u}}^a + \hat{\underline{u}}^d \end{aligned} \quad (27)$$

## ACKNOWLEDGEMENT

The authors would like to thank Michael Czarnetzki for programming support and Johannes Bunte for helpful discussions in deriving the equations in Sec. III and the Appendix.

## REFERENCES

- [1] T. Cover and J. Thomas, *Elements of Information Theory*. Wiley-Interscience New York, 2006.
- [2] M. Skoglund, N. Phamdo, and F. Alajaji, "Design and performance of VQ-based hybrid digital-analog joint source-channel codes," *Information Theory, IEEE Transactions on*, vol. 48, no. 3, pp. 708–720, Mar. 2002.
- [3] B. Chen and G. Wornell, "Analog error-correcting codes based on chaotic dynamical systems," *IEEE Transactions on Communications*, vol. 46, no. 7, pp. 881–890, Jul 1998.
- [4] P. Floor and T. Ramstad, "Noise analysis for dimension expanding mappings in source-channel coding," *IEEE 7th Workshop on Signal Processing Advances in Wireless Communications, 2006. SPAWC 2006.*, pp. 1–5, July 2006.
- [5] N. Wernersson, M. Skoglund, and T. Ramstad, "Polynomial based analog source-channel codes," *Communications, IEEE Transactions on*, vol. 57, no. 9, pp. 2600–2606, September 2009.
- [6] V. Vaishampayan and S. Costa, "Curves on a sphere, shift-map dynamics, and error control for continuous alphabet sources," *IEEE Transactions on Information Theory*, vol. 49, no. 7, pp. 1658–1672, July 2003.
- [7] S. Shamai, S. Verdú, and R. Zamir, "Systematic lossy source/channel coding," *Information Theory, IEEE Transactions on*, vol. 44, no. 2, pp. 564–579, Mar 1998.
- [8] U. Mittal and N. Phamdo, "Hybrid digital-analog (HDA) joint source-channel codes for broadcasting and robust communications," *IEEE Transactions on Information Theory*, vol. 48, no. 5, pp. 1082–1102, May 2002.
- [9] Z. Reznic, M. Feder, and R. Zamir, "Distortion bounds for broadcasting with bandwidth expansion," *Information Theory, IEEE Transactions on*, vol. 52, no. 8, pp. 3778–3788, Aug. 2006.
- [10] C. Hoelper and P. Vary, "Bandwidth efficient mixed pseudo analogue - digital speech transmission," in *Proceedings of European Signal Processing Conference (EUSIPCO)*. EURASIP, Sep. 2006.
- [11] S. M. Kay, *Fundamentals of Statistical Signal Processing: Estimation Theory*. Prentice-Hall Signal Processing Series, 1993.
- [12] J. Ohm and H. Lüke, *Signalübertragung: Grundlagen der digitalen und analogen Nachrichtenübertragungssysteme*. Springer, 2007.
- [13] T. Lookabaugh and R. Gray, "High-resolution quantization theory and the vector quantizer advantage," *Information Theory, IEEE Transactions on*, vol. 35, no. 5, pp. 1020–1033, sep 1989.